On Primary Incident Wave Models for Pyramidal Horn Gain Calculations

Gordon Mayhew-Ridgers, Johann W. Odendaal, *Member, IEEE*, and Johan Joubert, *Member, IEEE*

***Abstract*—A few widely used primary incident wave models for pyramidal horn antenna analysis are compared on the basis of gain calculations. The analysis is based on edge-wave diffraction theory, as presented in a recent publication, with some modifications made to the underlying theory. It is shown that these models agree well for high-gain horns with small flare angles, but that the differences are more profound for lower gain horns, where the flare angles are larger. The accuracy of the various models are studied by comparing the results to actual measurements. The respective effects of amplitude and phase variation in the primary incident wave are also illustrated.**

***Index Terms*—Antenna gain, horn antenna, primary incident wave.**

I. Introduction

MANY authors have proposed different methods to calculate the gain of pyramidal horn antennas [1]–[7]. Most of these analyses integrate the fields across the aperture of the horn. One of the main factors contributing to the accuracy of the aperture fields is the model used for the primary wave incident upon the aperture of the horn, resulting from the assumed source model. In this paper, some of the most often used models, as well as other derived models, are compared on the basis of gain calculations.

Calculations in this paper are based on an extension of a method proposed by Nye [4], where the fields in the aperture plane are composed of the primary incident wave, diffracted fields from the edges of the aperture, as well as reflected fields from inside the horn. Section II deals with the theoretical aspects of this study and also points out where the underlying theoretical model differs from that presented by Nye [4]. These modifications basically include the expressions used for the primary incident wave (which is different for each of the models studied within this paper); both the electric and magnetic fields in the aperture plane are used to determine the radiated far fields; slope diffracted fields are assumed to be negligible and the geometry for calculating the reflected fields from inside the horn is somewhat different. A proposed model for the amplitude variation of the primary incident wave is also included.

Section III compares numerical and measured results for pyramidal horn antennas with varying flare angles. It is shown that for horns with large flare angles the various models result in substantially different gain values, but that for horns with small flare angles the results are more comparable. From these results it is evident that some models fit both the results for high-gain (small flare angles) and low-gain (large flare angles) horns better than the rest of the models.

Section IV contains general conclusions that can be drawn from this study.

Manuscript received February 27, 1998; revised March 23, 1999.

The authors are with the Centre for Electromagnetism, Department of Electrical and Electronic Engineering, University of Pretoria, Pretoria 0002, South Africa.

Publisher Item Identifier S 0018-926X(00)07708-5.

II. Gain Calculations

Consider the pyramidal horn antenna of Fig. 1, excited via an incident TE_{10} mode with the electric field polarized along the y-axis. If it is assumed that the ohmic losses are negligible (in the order of 0.02 dB for a typical horn antenna [8]), the axial gain G can be expressed as

$$G = \frac{\pi}{\lambda^2 \eta} \frac{\left| \iint\limits_{S_\infty} (E_y^a - \eta H_x^a)\, ds \right|^2}{\mathrm{Re} \iint\limits_{S_a} [-E_y^a (H_x^a)^*]\, ds} \tag{1}$$

where

η intrinsic impedance of the propagation medium;
λ wavelength;
S_∞ aperture plane as shown in Fig. 1;
S_a aperture.

E_y^a and H_x^a are the electric and magnetic fields, tangential to the aperture plane, given by

$$E_y^a = \begin{cases} E_y^i + E_{y1}^d + E_{y2}^d + E_{y1}^{\mathrm{im}} + E_{y2}^{\mathrm{im}}, & y \le |b| \\ E_{y1}^d + E_{y2}^d, & y \ge |b| \end{cases} \tag{2}$$

and

$$H_x^a = \begin{cases} H_x^i + H_{x1}^d + H_{x2}^d + H_{x1}^{\mathrm{im}} + H_{x2}^{\mathrm{im}}, & y \le |b| \\ H_{x1}^d + H_{x2}^d, & y \ge |b|. \end{cases} \tag{3}$$

In these expressions E_y^i and H_x^i are the primary incident electric and magnetic fields, tangential to the aperture plane. E_{y1}^d and H_{x1}^d are the first-order diffracted electric and magnetic fields from edge 1, tangential to the aperture plane, while E_{y2}^d and H_{x2}^d are those from edge 2. E_{y1}^{im} and H_{x1}^{im} are the electric and magnetic fields, tangential to the aperture plane and are due to the images of edge 2 in the upper face of the horn. Similarly, E_{y2}^{im} and H_{x2}^{im} are those due to the images of edge 1 in the lower face of the horn.

As opposed to the analysis in [4], it is assumed that the slope diffracted fields from edges 3 and 4, as well as their reflections in the side faces of the horn, are negligible and can therefore be

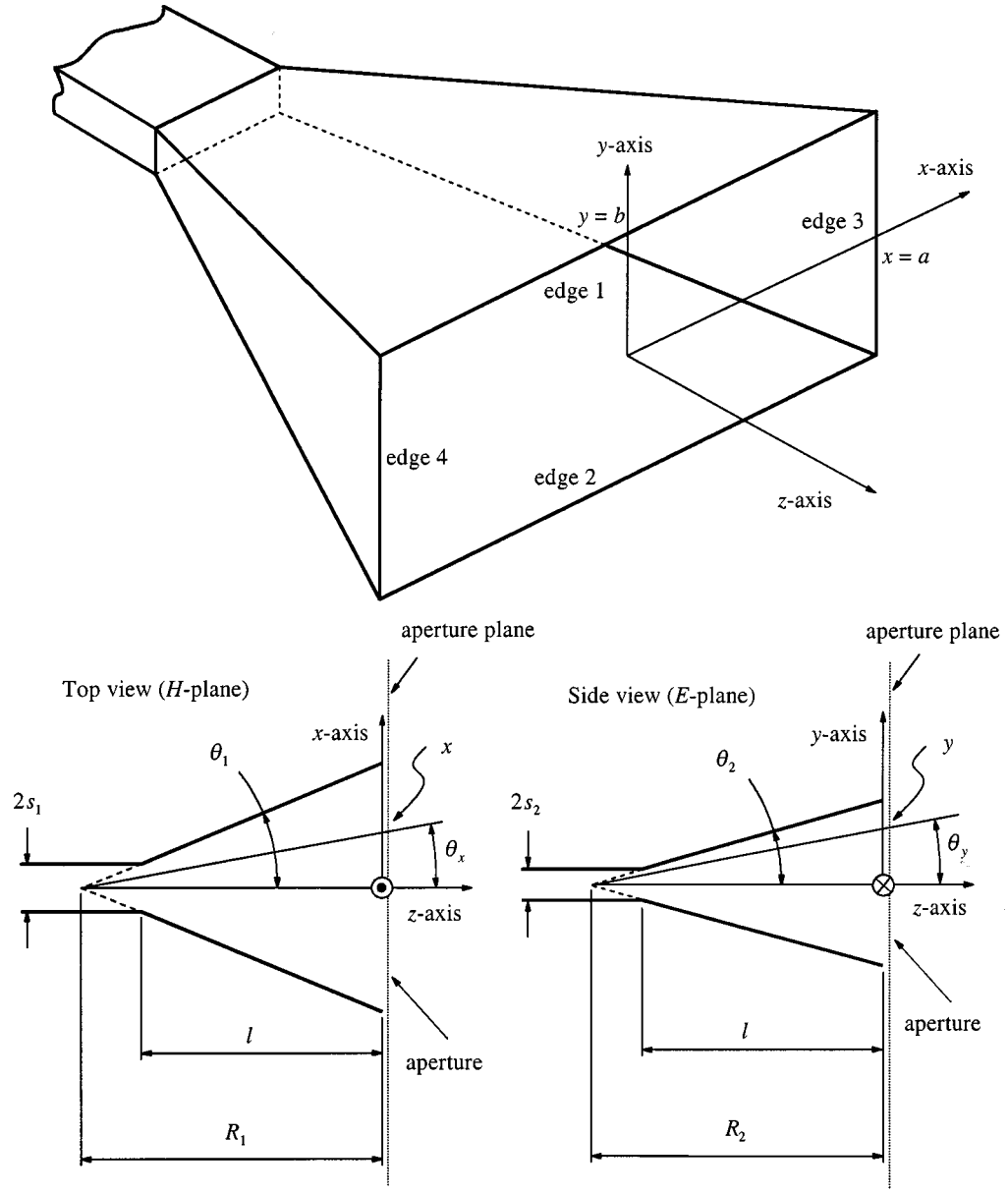

Fig. 1. Geometry of a pyramidal horn antenna.

omitted from this analysis.[1] This effectively limits the aperture plane to $(-a \le x \le a, -\infty < y < \infty, z = 0)$ as the fields are zero outside these limits. The expression in (1) for the gain also differs slightly from that given by Nye [4], in that both the electric and magnetic fields in the numerator are used to calculate the radiated far fields. The effect thereof becomes significant in cases where the width of the aperture is fairly narrow.

This paper is mainly concerned with the primary incident wave represented by E_y^i and H_x^i. For the purpose of this analysis these components can be expressed as

$$E_y^i(x, y) = A_E(x, y) \cos\left(\frac{\pi x}{2a}\right) e^{j\psi_E(x,y)} \tag{4}$$

[1]In [9], it is shown that for a typical horn antenna, only 0.0037% of the radiated power escapes around edges 3 and 4 as opposed to the 2.2% escaping around edges 1 and 2. It is therefore clear that slope diffraction can be ignored for the purpose of this analysis.

and

$$H_x^i(x, y) = \frac{-\beta}{\omega\mu} A_H(x, y) \cos\left(\frac{\pi x}{2a}\right) e^{j\psi_H(x,y)} \tag{5}$$

where μ is the permeability of the propagation medium and $\omega = 2\pi f$, with f the frequency. These expressions allow one to use different implementations for the amplitude and phase variations A_E, A_H, ψ_E, and ψ_H and, therefore, also make it possible to compare the different models on a similar basis. The electric and magnetic fields in the aperture are related by the leading term in (5), where β is the wave number in the aperture, given by

$$\beta = \sqrt{k^2 - \left(\frac{\pi}{2a}\right)^2} \tag{6}$$

with $k = 2\pi/\lambda$. By using this relation between the electric and magnetic fields in the aperture of the horn, it is furthermore

TABLE I
MODELS FOR AMPLITUDE AND PHASE VARIATIONS OF PRIMARY INCIDENT WAVE

Model	A_E	A_H	ψ_E	ψ_H
1	1	1	$kx^2/(2R_1) + ky^2/(2R_2)$	$kx^2/(2R_1) + ky^2/(2R_2)$
2	L/r	L/r	$\beta(r-L)$	$\beta(r-L)$
3	$\sqrt{\frac{R_1R_2}{(R_1+\delta_1)(R_2+\delta_2)}}\cos\theta_y$	$\sqrt{\frac{R_1R_2}{(R_1+\delta_1)(R_2+\delta_2)}}\cos\theta_x$	$\beta(r-L)$	$\beta(r-L)$
4	$\sqrt{\frac{R_1R_2}{(R_1+\delta_1)(R_2+\delta_2)}}\cos\theta_y$	$\sqrt{\frac{R_1R_2}{(R_1+\delta_1)(R_2+\delta_2)}}\cos\theta_x$	$\beta(\delta_1+\delta_2)$	$\beta(\delta_1+\delta_2)$
5	$\sqrt{\frac{R_1R_2}{(R_1+\delta_1)(R_2+\delta_2)}}\cos\theta_y$	$\sqrt{\frac{R_1R_2}{(R_1+\delta_1)(R_2+\delta_2)}}\cos\theta_x$	$\varphi_1+\varphi_2$	$\varphi_1+\varphi_2$

necessary to impose the condition that

$$A_E(0,0) = A_H(0,0) \tag{7}$$

in order to maintain the correct relation between the aperture fields.

The various models used for the amplitude and phase variations of the primary incident wave are summarized in Table I. In all the models, it is assumed that the amplitude of the primary incident electric field is unity in the center of the aperture and that the phase is zero there. The time-dependency is given by $\exp(-j\omega t)$.

Model 1 is based on the widely used amplitude and phase variations as given by Schelkunoff [1]. Nye [4] suggested the spherical amplitude and phase variations as implemented in Model 2. In Table I, the variable L is the harmonic mean of R_1 and R_2 given by

$$L = \frac{2}{R_1^{-1} + R_2^{-1}} \tag{8}$$

while

$$r = \sqrt{x^2 + y^2 + (L+z)^2}. \tag{9}$$

This is a good approximation if $R_1 \approx R_2$, but does not take into account that the primary incident wave tangential to the aperture is not equal to the total primary incident wave. In Model 3, a new model is proposed for the amplitude variation of the primary incident wave and is based on geometrical optics, as derived in the Appendix. The phase variation is still kept spherical to only illustrate the effects caused by the different amplitude variation. Here

$$\delta_1 = \sqrt{R_1^2 + x^2} - R_1 \tag{10}$$

and

$$\delta_2 = \sqrt{R_2^2 + y^2} - R_2. \tag{11}$$

In Model 4, the phase variations are replaced by a more accurate representation, as given by Maybell [5]. It differs from Schelkunoff's model in that (10) and (11) are not reduces to the normal quadratic expressions. Model 5 takes into account the fact that the wavelength changes as the wave propagates from the throat of the horn to the aperture, as given by Hawkins [6]. In this case the phase variations are given by

$$\varphi_1 = \left[2\pi \int_{-l}^{0} \frac{dz}{\lambda_g} + \frac{2\pi}{\lambda_g^w}(R_1 - l)\right]\left[\frac{1}{\cos\theta_x} - 1\right] \tag{12}$$

and

$$\varphi_2 = \left[2\pi \int_{-l}^{0} \frac{dz}{\lambda_g} + \frac{2\pi}{\lambda_g^w}(R_2 - l)\right]\left[\frac{1}{\cos\theta_y} - 1\right] \tag{13}$$

where λ_g is the wavelength in the aperture at position z and λ_g^w is the wavelength in the waveguide section.

The other field components E_{y1}^d, E_{y2}^d, H_{x1}^d, H_{x2}^d, E_{y1}^{im}, E_{y2}^{im}, H_{x1}^{im}, and H_{x2}^{im} can be calculated by following the analyses in [4], [10]–[12]. This paper follows the analysis in [10] and [11], where the geometry for calculating the images of edges 1 and 2 in the E-plane of the horn (for the calculation of E_{y1}^{im}, E_{y2}^{im}, H_{x1}^{im}, and H_{x2}^{im}), reflects the true geometry of the antenna (i.e., a circle in the E-plane with its center at $z = -R_2$). In [4], the images in the E-plane have been placed on a circle with its center at $z = -L$, which only works when $R_1 \approx R_2$. In Model 5, the variation of the wavelength inside the horn has also been accounted for in the calculation of E_{y1}^{im}, E_{y2}^{im}, H_{x1}^{im}, and H_{x2}^{im}. This has been done in a similar way to the analysis in [6] for the phase variation of the primary incident wave.

III. RESULTS

In order to illustrate the effect of each of the models presented in Table I, the gain values of three different pyramidal horn antennas were calculated and compared to measured results, as shown in Figs. 2–4. The results in Fig. 3 are for a Scientific-Atlanta Model 12-8.2 pyramidal horn antenna (medium horn), while the results in Figs. 2 and 4 are for horns with similar

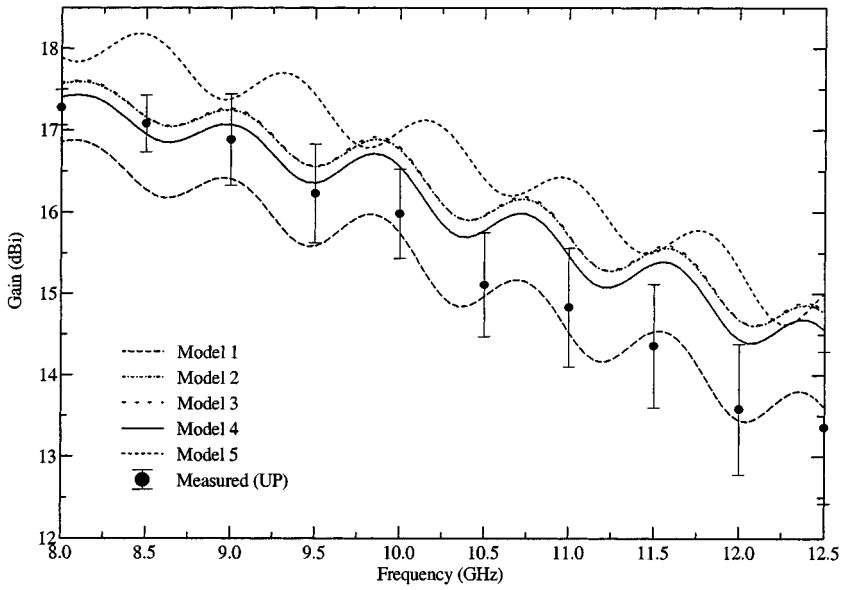

Fig. 2. Gain of short horn ($a = 96$ mm, $b = 73$ mm, $s_1 = 11.4$ mm, $s_2 = 5.1$ mm, $l = 150$ mm).

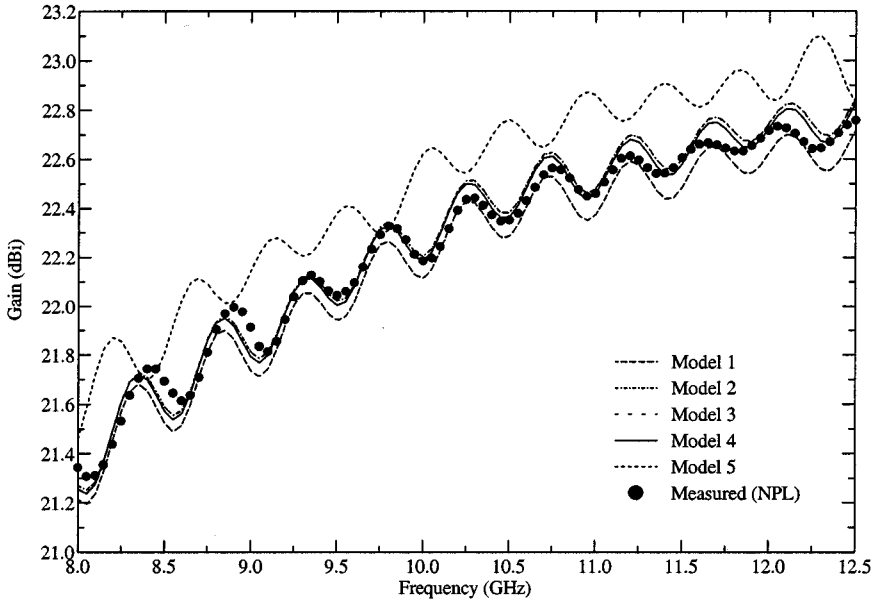

Fig. 3. Gain of medium horn ($a = 97.25$ mm, $b = 72$ mm, $s_1 = 11.43$ mm, $s_2 = 5.08$ mm, $l = 289$ mm).

aperture dimensions but with shorter (larger flare angles) and longer (smaller flare angles) axial lengths, respectively. For the short horn l was reduced to 150 mm and for the long horn l was increased to 430 mm. The measurements for the short horn were conducted in the compact antenna test range at the University of Pretoria (UP), South Africa, while the measured results for the Scientific-Atlanta Model 12-8.2 pyramidal horn antenna were obtained from the National Physical Laboratory (NPL), U.K. The error bars in Fig. 2 indicates the 3σ uncertainties, while the measured results in Fig. 3 are believed to be accurate to ± 0.05 dB which is the 2σ uncertainty.

It can be seen that the flare angles of the horns have a significant effect on the spread in gain values calculated with the different primary incident wave models. For the short horn the spread in gain values is more than 1.5 dB, while it is on the order of 0.1 dB for the long horn.

Evidently the phase variation of the fields in the aperture of the horn, has a more profound effect on the gain of the horn, than has the amplitude variation. It can be seen from Fig. 2 that if changing from one model to another also includes a new phase variation, there is a more significant effect than as only changing the amplitude variation.

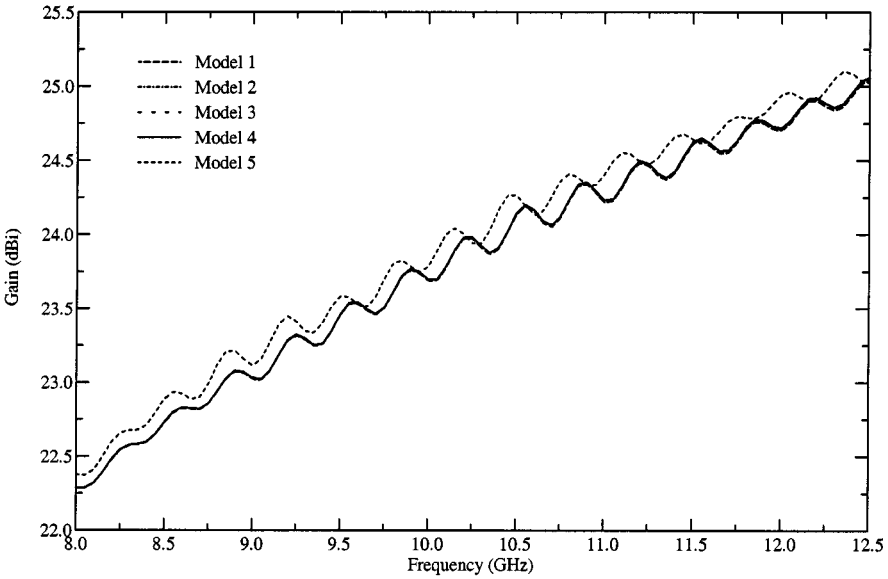

Fig. 4. Gain of long horn ($a = 97.25$ mm, $b = 72$ mm, $s_1 = 11.43$ mm, $s_2 = 5.08$ mm, $l = 430$ mm).

From the results in Fig. 2, it can be seen that Model 4 agrees quite well with the measured values for frequencies up to about 9.5 GHz. For frequencies above this the agreement is not as good, but the uncertainty in the measured values is higher and it is therefore difficult to make any real conclusions regarding the best model from Fig. 2.

In Fig. 3, there is much more agreement between the calculated results and the measured results. This can be explained by the smaller flare angles as opposed to those for the short horn, resulting in a less curved wavefront. It can be seen that Model 4 again fits the measured values very well and that Models 2 and 3 also result in fairly accurate values. It is clear, however, that Models 1 and 5 are not as accurate. In Fig. 3, the agreement between Models 2, 3, 4, and the measurements is better than 0.1 dB. This is also an improvement on the 0.2 dB agreement between theory and measurement as achieved by Nye [4] for the same antenna.

From the results in Fig. 4, it can be seen that there is hardly any difference between the models for pyramidal horn antennas with relatively small flare angles. Unfortunately, no measured results were available for the long horn. It is only Model 5 that results in gain values comparably higher than the other models. However, the results given by Hawkins [6] are also higher than those of other standard methods, which should be fairly accurate for high-gain horns.

IV. Conclusion

As was expected, this study has shown that the calculated gain values of pyramidal horn antennas are very much dependent on the model used for the primary wave incident upon the aperture of the horn, especially for horns with large flare angles. It was shown that for standard and longer horns (small flare angles) the various models result in approximately the same values, but that for extremely short horns (large flare angles) there are distinct differences in gain values. This is not surprising when keeping in mind that for large-flare horns, the phase departure is greater and the gain, therefore, becomes more sensitive to the details of the phase behavior on the aperture. It is clear that the amplitude variation of the primary incident wave (apart from the normal cosine distribution in the x-direction) does not have a significant effect on the calculated gain values. It is thus important to keep in mind what the effect of various approximations are, when analyzing these antennas. By taking into account the results of the previous section and the fact that the measurements in Fig. 3 are more accurate than those in Fig. 2, it is clear that Model 4 in general shows the best agreement with measured results.

The modifications made to the underlying theory, proposed by Nye [4], also proved to result in more accurate gain calculations. These modifications are the expressions used for the primary incident wave; both the electric and magnetic fields in the aperture plane are used to determine the radiated far fields; slope diffracted fields are assumed to negligible and the geometry for calculating the image fields is somewhat different.

It is quite surprising that Model 5 does not result in more accurate gain values as it is the most sophisticated of all the models. The most likely explanation for this is that the near-field phase center of the horn is not where it is thought to be and that the effect thereof is more profound on Model 5 than on the other models. In [13] it was indeed shown that the near-field phase center is closer to the aperture of the horn than is usually assumed. In [7] there is also numerical support for the existence of higher order modes in the horn aperture which have not been included in this analysis.

Appendix
Proposed Model for Primary Incident Wave Amplitude Variation

Consider the model depicted in Fig. 5 for the primary incident wave amplitude variation. It is assumed that the wavefront has two caustics, one at $z = -R_1$ and one at $z = -R_2$. By

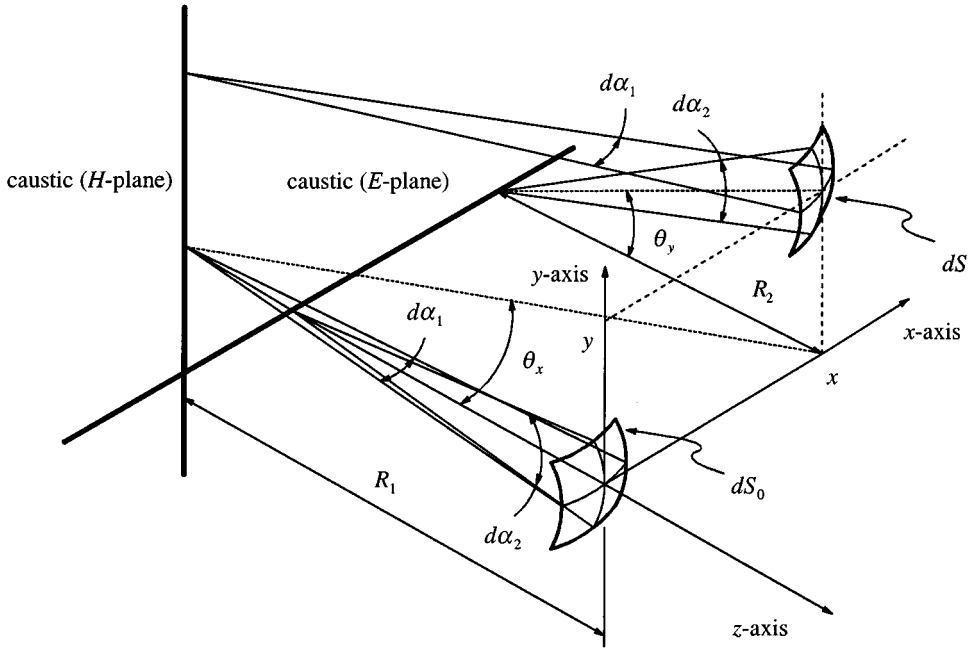

Fig. 5. Proposed model for primary incident wave amplitude variation.

following a geometrical optics approach, the fields on the two incremental surfaces, as shown in Fig. 5, are related by [14]

$$\frac{|E|}{|E_0|} = \sqrt{\frac{dS_0}{dS}} \tag{14}$$

where

E electric field at $(x, y, 0)$;
E_0 electric field at (0, 0, 0);
dS incremental surface on the wavefront at $(x, y, 0)$;
dS_0 incremental surface on the wavefront at (0, 0, 0).

Now dS can be written as

$$dS = (R_1 + \delta_1)(R_2 + \delta_2)\, d\alpha_1\, d\alpha_2 \tag{15}$$

where δ_1 and δ_2 are given by (10) and (11), while dS_0 can be written as

$$dS_0 = R_1 R_2\, d\alpha_1\, d\alpha_2. \tag{16}$$

This then implies that (14) can be written as

$$\frac{|E|}{|E_0|} = \sqrt{\frac{R_1 R_2}{(R_1 + \delta_1)(R_2 + \delta_2)}}. \tag{17}$$

It is important, however, to realize that as the field point in the aperture plane moves away from the center of the aperture, the electric and magnetic fields tangential to the aperture are not equal to the total fields in the aperture. In order to model this, (17) can be modified as

$$\frac{|E_y^a|}{|E_0|} = \sqrt{\frac{R_1 R_2}{(R_1 + \delta_1)(R_2 + \delta_2)}}\, \cos\theta_y \tag{18}$$

for the electric field tangential to the aperture plane and as

$$\frac{|H_x^a|}{|H_0|} = \sqrt{\frac{R_1 R_2}{(R_1 + \delta_1)(R_2 + \delta_2)}}\, \cos\theta_x \tag{19}$$

for the magnetic field tangential to the aperture plane.

ACKNOWLEDGMENT

The authors would like to thank D. G. Gentle of National Physical Laboratory (NPL), U.K., for his kind cooperation in providing the measured results of Fig. 3.

REFERENCES

[1] A. Schelkunoff and H. T. Friis, *Antennas: Theory and Practice*. New York: Wiley, 1952, pp. 515–535.
[2] L. Stutzman and G. A. Thiele, *Antenna Theory and Design*. New York: Wiley, 1981, pp. 397–415.
[3] C. A. Balanis, *Antenna Theory: Analysis and Design*, 2nd ed. New York: Wiley, 1997, pp. 651–695.
[4] F. Nye and W. Liang, "Theory and measurement of the field of a pyramidal horn," *IEEE Trans. Antennas Propagat.*, vol. 44, pp. 1488–1498, Nov. 1996.
[5] J. Maybell and P. S. Simon, "Pyramidal horn gain calculation with improved accuracy," *IEEE Trans. Antennas Propagat.*, vol. 41, pp. 884–889, July 1993.
[6] C. Hawkins and F. Thompson, "Modifications to the theory of waveguide horns," *Proc. Inst. Elect. Eng. Microwave Antennas Propagat.*, vol. 140, pp. 381–386, Oct. 1993.
[7] K. Liu, C. A. Balanis, C. R. Birtcher, and G. C. Barber, "Analysis of pyramidal horn antennas using moment methods," *IEEE Trans. Antennas Propagat.*, vol. 41, pp. 1379–1389, Oct. 1993.
[8] E. V. Jull, "Errors in the predicted gain of pyramidal horns," *IEEE Trans. Antennas Propagat.*, vol. AP-21, pp. 25–31, Jan. 1973.
[9] J. F. Nye, G. Hygate, and W. Liang, "Energy streamlines: A way of understanding how horns radiate backward," *IEEE Trans. Antennas Propagat.*, vol. 42, pp. 1250–1256, Sept. 1994.
[10] S. Yu, R. C. Rudduck, and L. Peters Jr., "Comprehensive analysis for E-plane of horn antennas by edge diffraction theory," *IEEE Trans. Antennas Propagat.*, vol. AP-14, pp. 138–149, Mar. 1966.

[11] G. Mayhew-Ridgers, "Accuracy of the gain-transfer method for aperture antenna gain measurements," M.Eng. thesis, Univ. Pretoria, Pretoria, South Africa, 1998.
[12] M. Born and E. Wolf, *Principles of Optics*, 6th ed. New York: Pergamon, 1989, pp. 556–592.
[13] J. W. Odendaal and C. W. I. Pistorius, "A method to measure the aperture field and experimentally determine the near-field phase center of a horn antenna," *IEEE Trans. Instrum. Meas.*, vol. 42, pp. 51–53, Feb. 1993.
[14] J. B. Keller, "Geometrical theory of diffraction," *J. Opt. Soc. Amer.*, vol. 52, pp. 116–130, 1962.

Gordon Mayhew-Ridgers was born in Ficksburg, South Africa, on February 11, 1973. He received the B.Eng., B.Eng.(honors), and M.Eng. degrees in electronic engineering from the University of Pretoria, South Africa, in 1994, 1996, and 1998, respectively. He is currently working toward the Ph.D. degree from the Department of Electrical and Electronic Engineering, University of Pretoria, where his current research interests include the analysis and design of new microstrip antenna elements and arrays.

From 1995 to 1997, he was with Telkom, South Africa, where he was mainly involved with the deployment of telecommunications network management systems. Since 1998, he has been with Vodacom, South Africa, where he is working on efficient spectrum utilization for wireless communications systems as well as network traffic modeling.

Johann W. Odendaal (S'89–M'95) was born in Frankfort, South Africa, in 1966. He received the B.Eng., M.Eng., and Ph.D. degrees in electronic engineering from the University of Pretoria, South Africa, in 1988, 1990, and 1993, respectively.

From 1993 to April 1994, he was with the ElectroScience Laboratory, Ohio State University, as a Visiting Scientist. Since May 1994, he has been with the University of Pretoria, where he is currently a Full Professor. His current research interests include electromagnetic scattering and radiation, compact range measurements and signal processing. He is also Director of the Centre for Electromagnetism, University of Pretoria. He has presented papers at international conferences and has also published a number of technical papers.

Dr. Odendaal is a member of the Antenna Measurement Techniques Association (AMTA) and a Registered Professional Engineer in South Africa.

Johan Joubert (M'86) received the B.Eng., M.Eng., and Ph.D. degrees in electronic engineering from the University of Pretoria, Pretoria, South Africa, in 1983, 1987, and 1991, respectively.

From 1984 to 1988, he was a Research Engineer with the National Institute for Aeronautical and Systems Technology, Council for Scientific and Industrial Research, Pretoria, South Africa. In May 1988, he joined the Department of Electrical and Electronic Engineering, University of Pretoria, where he is currently a Professor of electromagnetism. From July to December 1995, he was a Visiting Scholar in the Department of Electrical and Computer Engineering, California State University, Northridge. His research interests include computational electromagnetism and the analysis and design of passive microwave components and antenna arrays.